GDCh

Research Article

Angewandte
Chemie
International Edition
www.angewandte.org

Covalent Organic Frameworks

Mechanochemical Cyclotrimerization: A Versatile Tool to Covalent Organic Frameworks with Tunable Stacking Mode

Stefanie Hutsch, Allison Leonard, Sven Grätz, Mark Valentin Höfler, Torsten Gutmann, and Lars Borchardt*

Abstract: We introduce the first mechanochemical cyclotrimerization of nitriles, a facile strategy for synthesizing triazine-containing molecules and materials, overcoming challenges related to carbonization and solubility. Conducting this solid-state approach in a mixer ball mill with 4-Methylbenzonitrile, we synthesize Tris(4-methylphenyl)-1,3,5-triazine quantitatively in as little as 90 minutes. Just as fast, this mechanochemical method facilitates the synthesis of the covalent triazine framework CTF-1 using 1,4 Dicyanobenzene. Material characterization confirms its porous (650 m^{2}g^{-1}) and crystalline nature. Adjusting the induced mechanical energy allows control over the obtained stacking conformation of the resulting CTFs - from a staggered AB arrangement to an eclipsed AA stacking conformation. Finally, a substrate scope demonstrates the versatility of this approach, successfully yielding various CTFs.

Introduction

Cyclotrimerization reactions are encountered across various domains of chemistry, with particular significance arising in the synthesis of heterocycles, such as triazines or boroxines. These reactions are powerful tools in the production of large network structures, exemplified by the condensation-driven trimerization of 1,4-Phenylenediboronic acid to yield COF-1,[1] the triple aldol condensation leading to the formation of extensive covalent organic frameworks, including phenyl rings,[2] or the formation of Covalent Triazine Framework (CTF), primarily derived from the trimerization of

[*] S. Hutsch, A. Leonard, Dr. S. Grätz, Prof. Dr. L. Borchardt
     Department Inorganic Chemistry
     Ruhr-Universität Bochum
     Universitätsstrasse 150, 44801 Bochum, Germany
     E-mail: lars.borchardt@ruhr-uni-bochum.de

     M. V. Höfler, T. Gutmann
     Institute for Inorganic and Physical Chemistry
     Technical University Darmstadt
     Peter-Grünberg Strasse 8, 64287 Darmstadt, Germany
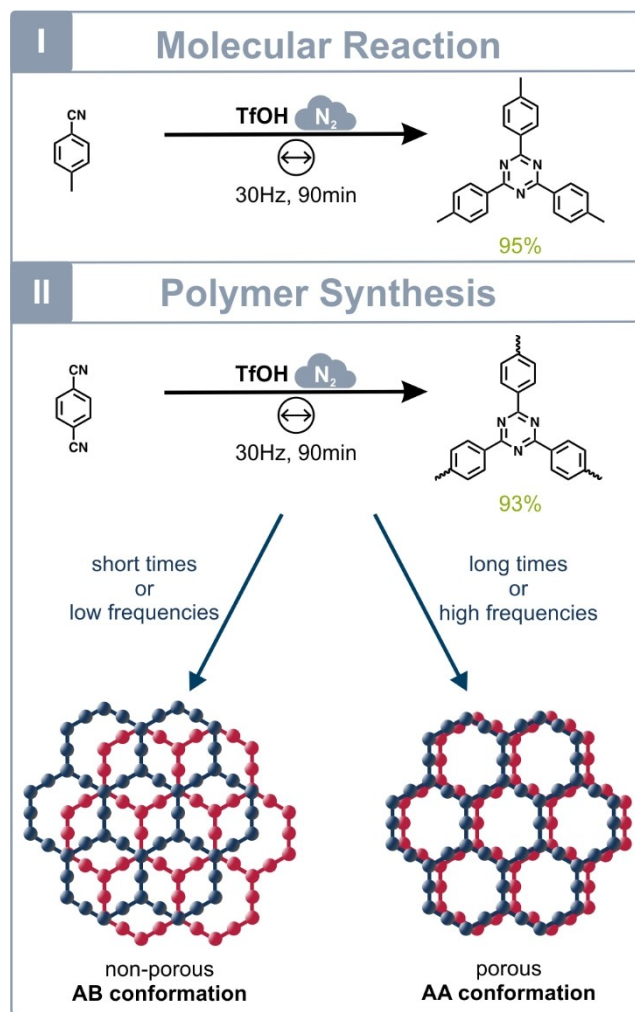
Figure 1. The mechanochemical reaction of 4-Methylbenzonitrile (MBN) to 2,4,6-Tris(4-methylphenyl)-1,3,5-triazine (TMPT) using Trifluoromethanesulfonic acid (TfOH) as catalyst yields 95% product. Utilizing the mechanochemical reaction of 1,4-Dicyanobenzene to mechanochemical covalent triazine framework (mCTF-1) was found to produce porous and non-porous material depending on the mechanical energy applied. The reaction parameters for both reactions were a 14 ml PFA vessel provided with a 15 mm ZrO$_2$ ball in a MM400 for 90 min, under nitrogen.

nitriles.[3,4] For the latter case, Kuhn et al. developed an ionothermal approach, involving the reaction of 1,4-Dicyanobenzene (DCB) within the melt of the Lewis acid ZnCl$_2$ for a duration of 40 hours.[3] The necessary elevated temper-

atures of 400 °C and even more, induce partial material carbonization, which, in turn, enhances porosity, however, decreases crystallinity, diminishes the nitrogen content and could lead to defects in the framework.[5] To circumvent this carbonization, an alternative approach involves dissolving DCB in chloroform and reacting it with the Brønsted acid Trifluoromethanesulfonic acid (TfOH).[6,7] This method not only reduces reaction times but also permits the use of lower temperatures compared to ionothermal synthesis.[6] However, the material obtained thereby exhibits a reduced specific surface area and suffers from incomplete polymerizations or structural defects.[8] A further limitation of this approach relates to the solvent selection, as it must be compatible with Trifluoromethanesulfonic acid.[9] Consequently, dichloromethane and chloroform are commonly utilized, which, however, constrains the choice of appropriate monomers owing to their solubility in these solvents. Despite this, the major problem with the use of solvents is the generation of extensive amounts of waste which we have to avoid in the interest of a more sustainable chemistry.[10]

Mechanochemistry, a solvent-free methodology, presents a promising avenue in cyclotrimerization reactions, offering the advantage of unrestricted monomer solubility and the environmental benefit of circumventing the generation of toxic waste associated with solvent use.[11] Numerous reactions, including photochemical reactions,[12] transition metal catalysis[13] as well as the synthesis of functional materials[14] and Scholl or Friedel–Crafts alkylation for porous organic polymer synthesis,[9,15,16] have been effectively adapted to the mechanochemical route.

In this study, we present the cyclotrimerization of nitriles within a ball mill for the first time – both for small molecules and large frameworks. The mechanochemical synthesis of CTFs (mCTFs) is rapid and can be conducted at room temperature, owing to the solvent-free protocol (Figure 1). Moreover, the modulation of various reaction parameters, including time, frequency, or temperature, enables the regulation of the stacking conformation from a staggered AB arrangement to an eclipsed AA stacking conformation

of the resulting CTFs by the induced mechanical energy. Additionally, the diversity of the mechanochemical cyclo-trimerization could be demonstrated by using diverse monomers leading to triazine-containing polymers.

Results and Discussion

Initially, the trimerization of 4-Methylbenzonitrile (1 eq.) was performed under nitrogen using Trifluoromethanesulfonic acid (4 eq.) in a 14 ml perfluoro alkoxy (PFA) polymer vessel equipped with one 15 mm Zirconium dioxide (ZrO_2) ball. The reaction took place in a MM400 mixer mill at 30 Hz for a duration of 90 minutes. Following the reaction, the crude product was neutralized with ammonia solution and washed with water, resulting in the isolation of 2,4,6-Tris(4-methylphenyl)-1,3,5-triazine (TMPT). The TMPT was obtained in a solid state, exhibiting a 95 % yield and underwent analytical characterization. The Fourier Transformation Infrared (FTIR) spectrum (Figure 2, I) revealed characteristic triazine bands at 1368 cm^{-1} and 1510 cm^{-1}, and the absence of the CN triple bond vibration band at 2220 cm^{-1} which highlights the achieved trimerization reaction of the carbonitriles and the purity of the product. In addition to the FTIR spectrum, the successful synthesis of TMPT was validated through the analysis of ^{1}H- and ^{13}C NMR spectra (Figure S1 and S2, ESI).

Subsequently, a comprehensive investigation of the influence of reaction time and frequency on the yield was conducted. Remarkably, after only 1 minute of reaction time, a yield of 66 % was observed, which further increased over an extended reaction duration (Figure 2, II). A similar trend was observed concerning frequency variation; at 10 Hz, the product yield was 72 %, and it increased with higher frequencies (Figure 2, III). This highlights the potential to transition trimerization into a mechanochemical approach, demonstrating the rapid nature achievable through the utilization of a ball mill.

Entry	Frequency (Hz)	Yield (%)
1	10	72
2	15	91
3	20	90
4	25	99
5	30	95
6	35	99
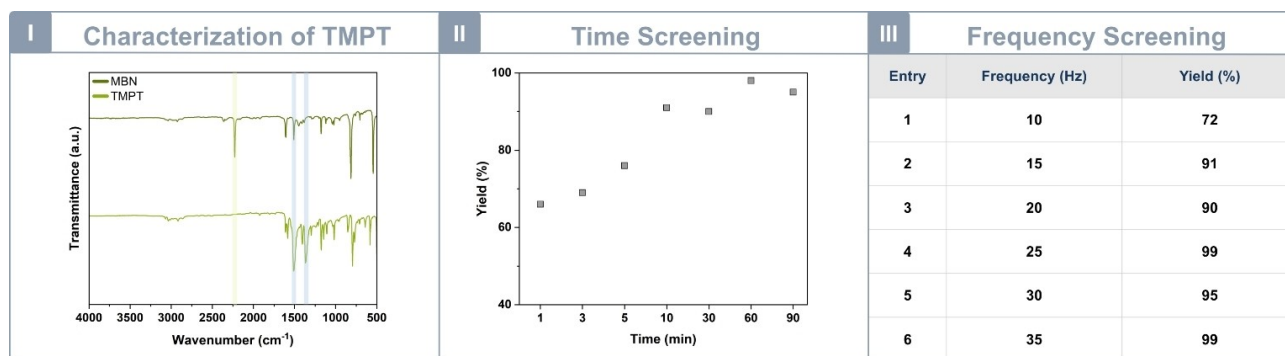
Figure 2. Characterization and results of the time and frequency screening of TMPT: I) FTIR spectrum of MBN (olive) and TMPT (green). The C≡N band is marked in light green at 2220 cm^{-1} and the characteristic triazine bands are marked in light blue. II) The yields of the time screening (black framed grey dots) of the obtained TMPT illustrate a rise with increased time. The reactions took place in a 14 ml PFA vessel equipped with a 15 mm ZrO$_2$ ball in a MM400 at 30 Hz, under nitrogen. III) The frequency screening displays a low yield for 10 Hz increasing with enhanced frequencies. The reactions occurred in a 14 ml PFA vessel provided with a 15 mm ZrO$_2$ ball in a MM400 for 90 min, under nitrogen. For the experiment at 35 Hz, the reaction was conducted using an MM500 mixer mill by Retsch with the same parameters.

Having successfully accomplished the cyclotrimerization of 4-Methylbenzonitrile to obtain TMPT as a "proof-of-principle" reaction, the subsequent phase involved the conversion into a covalent triazine framework. We maintained the same standard parameters, with a 90-minute reaction duration and a frequency of 30 Hz. Therefore, we replaced 4-Methylbenzonitrile with 1,4-Dicyanobenzene (DCB). The process for isolating the pure product was modified. It initially included a washing step in ammonia solution, and subsequent washing with acetonitrile using an ultrasonic bath. The product was washed sequentially with acetone and ethanol, and the resulting solid was dried at 80 °C overnight.

The product underwent characterization via FTIR analysis. As observed previously, the characteristic triazine bands were clearly evident at 1350 cm^{-1} and 1505 cm^{-1}, while the C≡N vibration at 2220 cm^{-1} (Figure 3, I) ceased to be detected, thereby confirming the successful synthesis of the triazine material.

^{13}C cross polarization magic angle spinning (CP MAS) NMR reveals peaks of the aromatic carbons (b and c) at 138.5 ppm and 128.5 ppm. The signal at 171.6 ppm belongs to the carbons inside the triazine ring and the small peak at 115.1 ppm can be assigned to terminal C≡N groups[17] (Figure S3, additional: Figure S4, ESI) further validating the accomplished synthesis of the CTF. In addition, the first ^{15}N CP MAS NMR spectrum enhanced by dynamic nuclear polarization (DNP) was measured for this material (Figure 3, IV). The strongest peak at 216.6 ppm is clearly assigned to the nitrogen of the triazine ring (a) and the signal at 64.9 ppm refers to the terminal nitrile group (b). These observations clearly support the formation of the triazine material. It further shows that the sample contains some remaining terminal C≡N.

X-ray photoelectron spectroscopy (XPS) measurements were employed to validate the presence of aromatic carbons, evident through a peak at 284.5 eV, corresponding to sp^2 carbons (Figure S6, ESI). Another peak indicated the presence of carbons bonded to the nitrogen within the triazine ring, with a binding energy of 286.9 eV (Figure S6, ESI). This was further substantiated by a nitrogen scan (Figure S7, ESI), revealing a signal at 398.6 eV, attributed to the C≡N bond. Elemental analysis (EA) was performed, revealing a C/N ratio of 4.01 (Table S1, ESI), which is nearly ideal compared to the calculated C/N ratio of 4. This finding highlights that there was no carbonization observed for the mechanochemical approach.

The energy-dispersive X-ray (EDX) spectrum and mapping (Figure S8, S9 and Table S1, ESI), confirm the absence of residual Trifluoromethyl sulfonic acid in the material. Further, the Scanning Electron Microscopy (SEM) image illustrates the layered material seen in Figure 3, VI.

Subsequently, physisorption measurements were conducted to evaluate the material's porosity. The specific surface area (SSA$_{BET}$) for N$_2$ physisorption was quantified at 585 m^2 g^{-1}, (Figure 3, II) illustrated by a type I isotherm
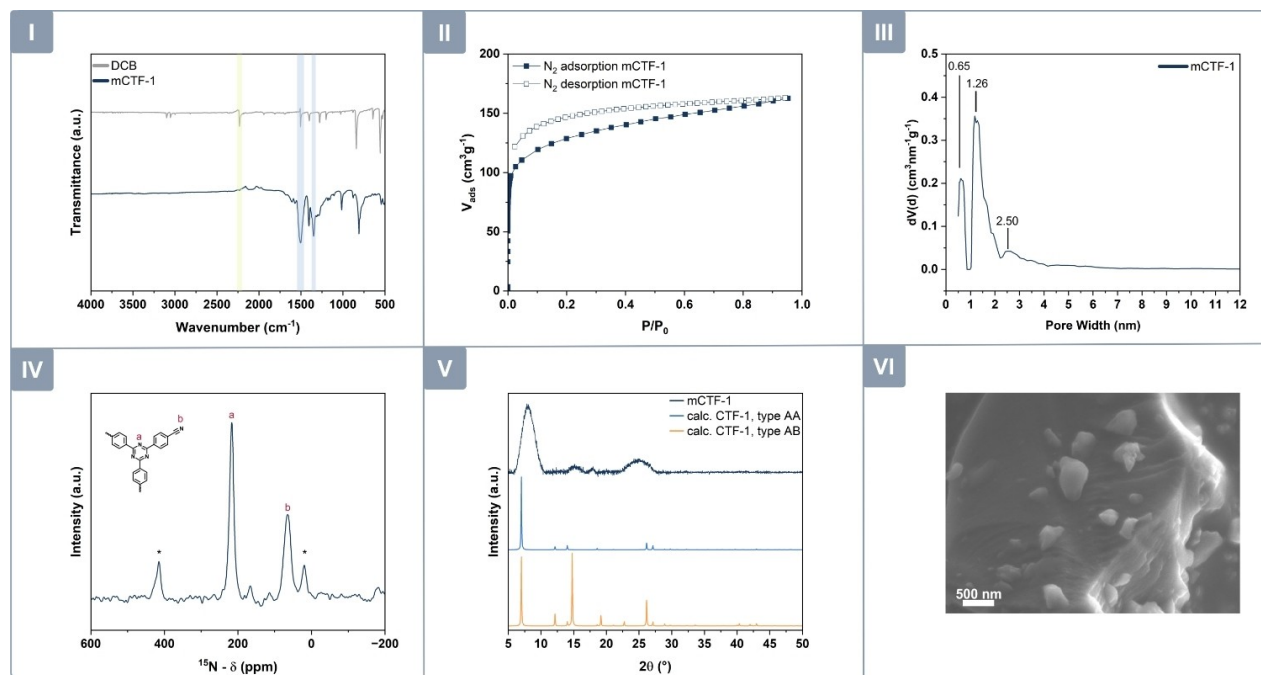
Figure 3. Characterization of mCTF-1: I) FTIR of DCB (grey) and mCTF-1 (dark blue). The C≡N band is marked in light green at 2220 cm^{-1} and the triazine bands are marked in light blue at 1505 and 1350 cm^{-1}; II) N$_2$ physisorption isotherm at 77 K. III) Pore size distribution, slit pore NLDFT equilibrium model; IV) DNP enhanced ^{15}N CP MAS spectrum measured at 8 kHz spinning at 120 K. The isotropic signals at 64.9 ppm and 216.6 ppm are labelled with letters (a and b), and signals marked with asterisk are spinning side bands. Note: The sample was prepared by impregnating 10 mg of the sample with 10 μl of a 15 mM solution of bTbK in TCE; V) PXRD pattern within the range of 5°–50° of mCTF-1 in dark blue and the calculated patterns of CTF-1 with an eclipsed stacking mode AA in blue and the staggered mode AB in orange; VI) SEM image with a scale of 500 nm at 5 kV accelerating voltage.

indicating a microporous structure. Further insight was gained through Argon and CO_2 physisorption measurements. The pore size distribution (Figure 3, III) reveals pores mainly the size of 0.65 nm and 1.26 nm and partly mesopores <3.5 nm. Moreover, Argon measurements results in a SSA_{BET} of 307 $m^2 g^{-1}$ and a CO_2 uptake of 50.7 mmol g^{-1} at 273 K, respectively (Figure S10 and S11, ESI).

Furthermore, in order to investigate the morphological aspects of the porous material, we conducted powder X-ray diffraction (PXRD) analysis, which unveiled a crystalline nature of an AA stacked CTF-1 (Figure 3, V), as evidenced by a pronounced peak associated with the (100) reflection at $2\theta = 7.8°$. Two signals were examined at $2\theta = 15.1°$ and $2\theta = 17.9°$, corresponding to the (110) and (200) reflections.[3,17] Additionally, the peak observed at $2\theta = 24.9°$ can be attributed to the interlayer (001) stacking. In contrast to the calculated PXRD patterns (Figure 3, V), we observe a slight shift in the experimental data. The reason could be a difference in the interlayer distance, which could influence the stacking and, thus, the pattern.[18]

Additionally, the optoelectronic property of the mCTF-1 was investigated via UV/Vis diffuse reflectance spectroscopy (DRS). Utilizing the Kubelka–Munk method and the Tauc plot, an electron band gap of 3.22 eV was determined (Figure S13, ESI), which is slightly increased compared to values in literature (2.94 eV),[19] rendering the porous material intriguing for potential applications in photocatalysis.

Finally, the material's thermal stability was assessed via thermal gravimetric analysis (Figure S14, ESI), revealing its exceptional stability up to 630 °C.

Moving on to gain deeper insights into the mechanochemical reaction, we conducted both a time and frequency screening. Beginning with the time screening, we varied the reaction durations to 1, 3, 5, 10, 30, and 60 minutes, all at a fixed frequency of 30 Hz. By observing the yield, seen in Figure 4, I up, we notice a remarkable increase from 40 % at 1 minute to a yield exceeding 99 % at 90 minutes. Notably, it became apparent that porosity began to develop after 10 minutes of reaction, and the SSA_{BET} increased progressively with time.
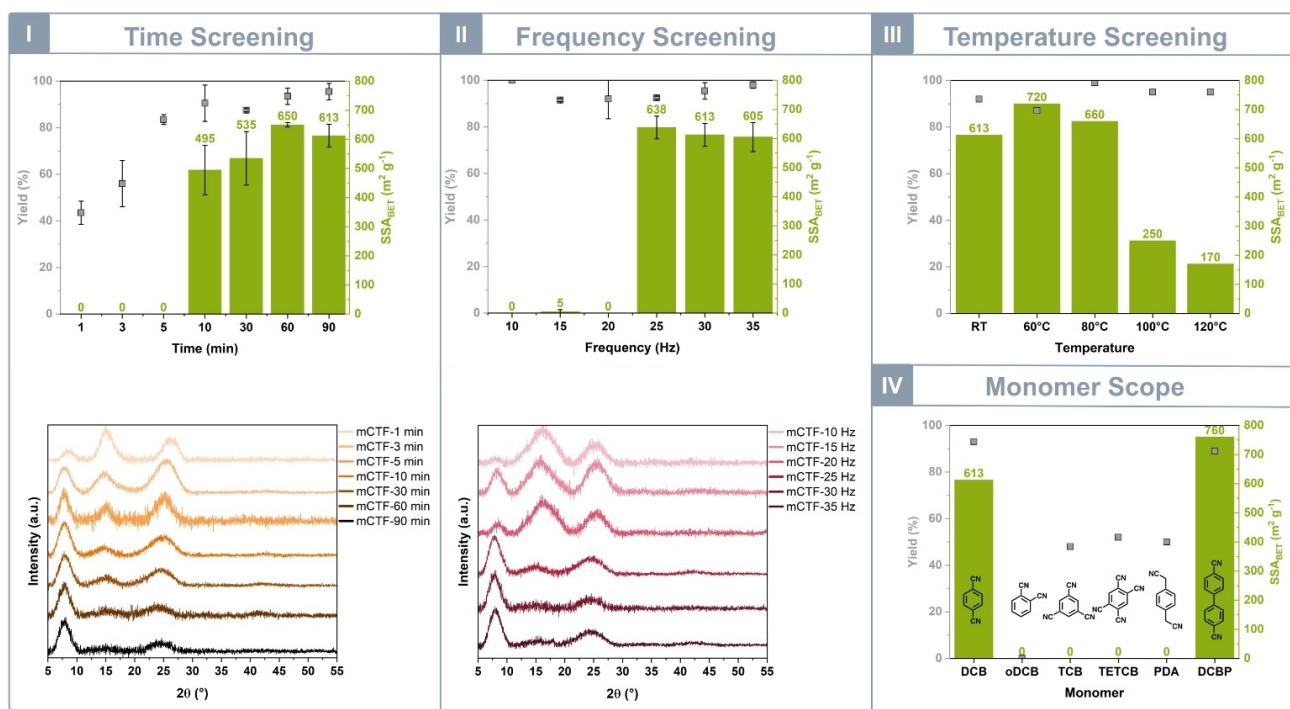
Figure 4. The parameter screening: I) Time screening; up: SSA_{BET} (green columns) and yields (black framed grey dots) of the obtained mCTFs illustrating a rise in yield and SSA_{BET}, using reaction times over 10 min, with increasing time and non-porous polymer at lower times than 10 min; bottom: PXRD patterns of the obtained mCTFs of the time screening. The reactions took place in a 14 ml PFA vessel provided with a 15 mm ZrO_2 ball in a MM400 at 30 Hz, under a N_2 atmosphere. II) Frequency screening; up: SSA_{BET} (green columns) and yields (black framed grey dots) of the obtained mCTFs illustrating a high yield for all, non-porous polymers at 10, 15 and 20 Hz and a strong increase for higher frequencies; bottom: PXRD patterns of the obtained mCTFs of the frequency screening. The reactions took place in a 14 ml PFA vessel provided with a 15 mm ZrO_2 ball in a MM400 for 90 min, under a N_2 atmosphere. For the experiment at 35 Hz, the reaction was conducted using an MM500 mixer mill by Retsch with the same parameters. III) Temperature screening of the cyclotrimerization of DCB and the impact on the SSA_{BET} (green columns) and the yield (black framed grey dots) of the synthesized mCTFs. The reactions occurred in a 14 ml PFA vessel provided with a 15 mm ZrO_2 ball in a MM400 for 90 min at 30 Hz, under a N_2 atmosphere. IV) Substrate scope of the cyclotrimerization, illustrating the SSA_{BET} (green columns) and the yield (black framed grey dots) of the synthesized mCTFs. The reactions took place in a 14 ml PFA vessel equipped with a 15 mm ZrO_2 ball in a MM400 for 90 min at 30 Hz, under a N_2 atmosphere.

The frequency screening involved the use of frequencies ranging from 10 to 35 Hz for a fixed duration of 90 minutes, and for all frequencies high yields were obtained (Figure 4, II up). Regarding SSA_{BET}, we observed a non-porous nature with the materials produced at 10, 15, and 20 Hz as we seen for short reaction times before.

Comparing the PXRD patterns from the time screening (Figure 4, I bottom), it is evident that changes occurred over time. The peak at $2\theta = 15.1°$ diminished until it was nearly absent after 90 minutes, and the peak at $2\theta = 24.3°$ also exhibited a reduction in intensity. A similar trend was observed in the frequency screening in Figure 4, II bottom. In both cases, alterations in crystallinity were apparent. The prominent intensity of the peak at $2\theta = 15.1°$ and the reduced intensity of the (100) reflection typify CTF-1 as possessing a staggered AB conformation. This may explain the significant differences in material porosity: the AB stacking mode of CTF-1 is known to have low porosity due to sheet overlap that impedes pore development. Conversely, the AA stacked CTF-1 material is porous, aligning with our experimental findings. It is known that CTF-1 synthesized with Trifluoromethanesulfonic acid as a catalyst is more likely to adopt the staggered AB conformation. This preference arises due to the strong interaction between TfOH and the assembled triazine ring, inducing a twist between the layers and resulting in the staggered stacking conformation.[20,21] This is also evident in the different dissociative adsorption (E_{ads}) and interlayer interaction energies (E_{int}), which are $E_{ads} = -106$ kJ mol^{-1} and $E_{int} = -327$ kJ mol^{-1} for the AA conformation, and $E_{ads} = -135$ kJ mol^{-1} and $E_{int} = -322$ kJ mol^{-1} for the AB conformation.[21] High temperatures of above 350°C or mechanochemical treatment with KOH/LiOH can disrupt this interaction by surpassing the dissociative adsorption energies, thereby causing the layers to shift into an eclipsed stacking mode.[20,21] Therefore, we assume a minimum of mechanical force (≤ 10 min or ≤ 25 Hz) is required to disrupt the interaction between the acid catalyst and the triazine ring, to obtain the eclipsed AA conformation. Moreover, ball milling is recognized for its capability in exfoliation.[22] Depending on the direction and force acting on the bulk material, the shear force induced by ball milling can achieve exfoliation.[22] It is conceivable that the shear force could induce a shift in the CTF-1 layers, resulting in an eclipsed conformation.

In validating the hypothesis, the experimental configuration was transferred to a resonant acoustic mixer (RAM), which ensures good mixing without the ball.[23] Therefore, a similar set-up was applied at diverse accelerations ranging from 50 g to 90 g. The yields showed an increase from 81% using 50 g to exceeding 99% at 90 g (Figure S15, ESI). In contrast to ball mills, however, the polymers acquired through RAM were all non-porous and exhibited a staggered AB conformation. Thus, confirming the mechanical force generated by the ball is required to disrupt the interaction between the triazine moiety and the TfOH, resulting in the eclipsed conformation.

Furthermore, the temperature impact was examined. The porosity increased when the temperature was raised to 60°C (mCTF-60°C) and 80°C (mCTF-80°C). However, further temperature elevation to 100°C (mCTF-100°C) and 120°C (mCTF-120°C) resulted in reduced porosity (Figure 4, III) Once more, the PXRD pattern revealed a conformational change from eclipsed for mCTF-60°C and mCTF-80°C to staggered for mCTF-100°C and mCTF-120°C. Given that the interaction between the triazine moiety and TfOH is responsible for the AB conformation, and the disruption of this interaction leads to the AA arrangement, it seems counterintuitive at first that a conformational change from AA to AB occurs with increasing temperature. A hypothesis could be the formation of a TfOH dimer at higher temperatures, resulting in more TfOH molecules in an unit cell, favoring the AB conformation. Consequently, the dissociative adsorption energy changes significantly: $E_{ads} = -207$ kJ mol^{-1} and $E_{int} = -428$ kJ mol^{-1} for the AA conformation, and $E_{ads} = -256$ kJ mol^{-1} and $E_{int} = -443$ kJ mol^{-1} for the AB conformation.[21] Therefore, we may observe changes in the conformation from AA to AB for mCTF-100°C and mCTF-120°C leading to a decreasing specific surface area.

Nevertheless, the XPS survey (Figure S5) revealed a carbon-fluor signal which indicates contamination with PFA abrasion of the vessel material in the porous triazine framework. Therefore, various materials were investigated to avoid material abrasion during milling. ZrO_2 is a well-established material in mechanochemical synthesis of porous polymers.[15] Starting with milling jars made of ZrO_2, which involved a volume change from 14 ml to 25 ml and an additional 15 mm ZrO_2 ball, resulted in a porous polymer similar to mCTF-1. The obtained porous polymer (mCTF-MM400-ZrO_2) exhibited a slightly enhanced SSA_{BET} of 660 m^2 g^{-1} and achieved a yield of 97% (Figure S16, ESI). XPS measurements revealed the absence of Zr residue in the polymer (Figure S17, ESI), confirming no abrasion in this case.

To further examine the applicability, we proceeded to the planetary ball mill, the P7 by Fritsch, and the influence of silicon nitride (Si_3N_4) in conjunction with ZrO_2. The vessel volume underwent an adjustment, reducing from 25 ml to 20 ml, and the balls were changed to three 10 mm ZrO_2 balls due to the jar form. The resultant polymer from the ZrO_2 material (mCTF–P7-ZrO_2) exhibited comparability with mCTF-1 and mCTF-MM400-ZrO_2. The SSA_{BET} of mCTF–P7-ZrO_2 reached 585 m^2 g^{-1}, achieving a slightly reduced yield of 81%. In contrast, utilization of the less dense material Si_3N_4 led to a lower specific surface area of 230 m^2 g^{-1} but ensured a complete conversion (Figure S16, ESI). A possible hypothesis could be that the polymer stacking arrangement deviates from a strict AA conformation and instead represents a mixture of AA and AB configurations. This observation provides insight into the comparatively reduced SSA_{BET}. Furthermore, this demonstrates the broad applicability of the cyclotrimerization reaction for different types of ball mills and milling materials.

Thus far, the mechanochemical reaction of 1,4-Dicyanobenzene with Trifluoromethanesulfonic acid has been investigated, encompassing the screening of various parameters

Angew. Chem. Int. Ed. **2024**, *63*, e202403649 (5 of 7)

© 2024 The Authors. Angewandte Chemie International Edition published by Wiley-VCH GmbH

and the analysis of different aspects of the porous material. Moving on to the variety of the cyclotrimerization process by exploring a range of substrates with the aim to synthesize porous triazine-containing polymers (Figure 4, IV) Consequently, nitriles were selected, featuring diverse nitrile group amount and positions.

Beginning with an ortho-substituted monomer, the formation of a polymer did not occur. Instead, gas development was observed, suggesting a competitive reaction in which the condensation of nitrile groups might produce cyanogen (C_2N_2) as a byproduct.[24] Additionally, the use of monomers containing more than 2 CN groups, 1,3,5-Tricyanobenzene (TCB) and 1,2,4,5-Tetracyanobenzene (TETCB), revealed the formation of a non-porous triazine containing polymer. Comparable outcomes were achieved with a para substituted non-conjugated monomer, 2,2′-(1,4-Phenylene) diacetonitrile (PDA).

An excellent yield and a high porosity were attained with a para-substituted aromatic nitrile, 4,4'-Biphenyldicarbonitrile (BPDC) which is similar to the distinguished results of the mCTF-1 made of DCB.

Conclusion

In summary, we developed the first mechanochemical cyclotrimerization of nitriles using Trifluoromethanesulfonic acid, within a ball mill facilitating the synthesis of small molecules such as Tris(4-methylphenyl)-1,3,5-triazine as well as large triazine frameworks, referred here as mCTF. Notably, the resulting covalent triazine framework exhibited crystallinity and porosity. Extensive screenings were conducted to understand this mechanochemical reaction, exploring time, frequency, and temperature dependencies. During the screening of parameters including reaction times, frequencies, and temperature, we observed a change in the conformation of the CTF-1. Low mechanical energy input, such as low reaction times or frequencies, leads to the formation of less porous polymers with a staggered AB arrangement, while a higher input results in the eclipsed AA conformation. Additionally, increasing the reaction temperature induced a conformational change from AA to AB, assuming that dimerization of the Trifluoromethanesulfonic acid plays a crucial role. Optimization efforts involved investigating different materials and mill types to reduce PFA jar abrasion. Moreover, we accomplished the successful synthesis of various covalent triazine frameworks using this mechanochemical method, utilizing different aromatic nitriles as monomeric precursors.

Supporting Information

Supporting Information is available from the Wiley Online Library or from the author.

Conflict of Interest

The authors declare no conflict of interest.

Data Availability Statement

The data supporting the findings of this study are available in the article and its supplementary material.

Keywords: Cyclotrimerization · Mechanochemistry · Covalent Triazine Framework · NMR spectroscopy

[1] a) A. P. Côté, A. I. Benin, N. W. Ockwig, M. O'Keeffe, A. Matzger, O. M. Yaghi, *Science* **2005**, *310*, 1166; b) A. M. Evans, I. Castano, A. Brumberg, L. R. Parent, A. R. Corcos, R. L. Li, N. C. Flanders, D. J. Gosztola, N. C. Gianneschi, R. D. Schaller, et al., *J. Am. Chem. Soc.* **2019**, *141*, 19728.

[2] a) M. Rose, N. Klein, I. Senkovska, C. Schrage, P. Wollmann, W. Böhlmann, B. Böhringer, S. Fichtner, S. Kaskel, *J. Mater. Chem.* **2011**, *3*; b) F. M. Wisser, K. Eckhardt, D. Wisser, W. Böhlmann, J. Grothe, E. Brunner, S. Kaskel, *Macromolecules* **2014**, *47*, 4210; c) F. Wisser, K. Eckhardt, D. Wisser, W. Böhlmann, J. Grothe, E. Brunner, S. Kaskel, *Macromolecules* **2014**, *47*.

[3] P. Kuhn, M. Antonietti, A. Thomas, *Angew. Chem.* **2008**, *120*, 3499.

[4] D. Kong, X. Han, J. Xie, Q. Ruan, C. D. Windle, S. Gadipelli, K. Shen, Z. Bai, Z. Guo, J. Tang, *ACS Catal.* **2019**, *9*, 7697.

[5] a) L. Liao, M. Li, Y. Yin, J. Chen, Q. Zhong, R. Du, S. Liu, Y. He, W. Fu, F. Zeng, *ACS Omega* **2023**, *8*, 4527; b) Y. Zhang, S. Jin, *Polymer* **2018**, *11*.

[6] S. Ren, M. J. Bojdys, R. Dawson, A. Laybourn, Y. Z. Khimyak, D. J. Adams, A. I. Cooper, *Adv. Mater.* **2012**, *24*, 2357.

[7] a) J. Liu, W. Zan, K. Li, Y. Yang, F. Bu, Y. Xu, *J. Am. Chem. Soc.* **2017**, *139*, 11666; b) A. Bhunia, I. Boldog, A. Möller, C. Janiak, *J. Mater. Chem. A* **2013**, *1*, 14990.

[8] J. Artz, *ChemCatChem* **2018**, *10*, 1753.

[9] E. Troschke, S. Grätz, T. Lübken, L. Borchardt, *Angew. Chem. Int. Ed.* **2017**, *56*, 6859.

[10] T. Friščić, C. Mottillo, H. M. Titi, *Angew. Chem. Int. Ed.* **2020**, *59*, 1018.

[11] W. Jones, M. D. Eddleston, *Faraday Discuss.* **2014**, *170*, 9.

[12] D. M. Baier, C. Spula, S. Fanenstich, S. Grätz, L. Borchardt, *Angew. Chem. Int. Ed.* **2023**, *62*, e202218719.

Angew. Chem. Int. Ed. **2024**, *63*, e202403649 (6 of 7)

© 2024 The Authors. Angewandte Chemie International Edition published by Wiley-VCH GmbH

[13] a) W. Pickhardt, C. Beaković, M. Mayer, M. Wohlgemuth, F. J. L. Kraus, M. Etter, S. Grätz, L. Borchardt, *Angew. Chem. Int. Ed.* **2022**, *61*, e202205003; b) W. Pickhardt, E. Siegfried, S. Fabig, M. F. Rappen, M. Etter, M. Wohlgemuth, S. Grätz, L. Borchardt, *Angew. Chem. Int. Ed.* **2023**, *62*, e202301490; c) C. G. Vogt, M. Oltermann, W. Pickhardt, S. Grätz, L. Borchardt, *Adv Energy Sustain Res* **2021**, *2*, 2100011.

[14] T. Rensch, V. Chantrain, M. Sander, S. Grätz, L. Borchardt, *ChemSusChem* **2022**, *15*, e202200651.

[15] A. Krusenbaum, S. Grätz, S. Bimmermann, S. Hutsch, L. Borchardt, *RSC Adv.* **2020**, *10*, 25509.

[16] a) A. Krusenbaum, J. Geisler, F. J. L. Kraus, S. Grätz, M. V. Höfler, T. Gutmann, L. Borchardt, *J. Polym. Sci.* **2022**, *60*, 62; b) A. Krusenbaum, F. J. L. Kraus, S. Hutsch, S. Grätz, M. V. Höfler, T. Gutmann, L. Borchardt, *Adv. Sustainable Syst.* **2023**, 2200477.

[17] S. Kuecken, A. Acharjya, L. Zhi, M. Schwarze, R. Schomäcker, A. Thomas, *Chem. Commun.* **2017**, *53*, 5854.

[18] K. S. Rawat, S. Borgmans, T. Braeckevelt, C. V. Stevens, P. van der Voort, V. van Speybroeck, *ACS Appl. Nano Mater.* **2022**, *5*, 14377.

[19] J. Bi, W. Fang, L. Li, J. Wang, S. Liang, Y. He, M. Liu, L. Wu, *Macromol. Rapid Commun.* **2015**, *36*, 1799.

[20] J. Fan, X. Suo, T. Wang, Z. Wang, C.-L. Do-Thanh, S. M. Mahurin, T. Kobayashi, Z. Yang, S. Dai, *J. Mater. Chem. A* **2022**, *10*, 14310.

[21] J. Liu, P. Lyu, Y. Zhang, P. Nachtigall, Y. Xu, *Adv. Mater.* **2018**, *30*.

[22] A. Tayyebi, N. Ogino, T. Hayashi, N. Komatsu, *Nanotechnology* **2020**, *31*, 75704.

[23] M. Wohlgemuth, S. Schmidt, M. Mayer, W. Pickhardt, S. Grätz, L. Borchardt, *Chem* **2023**, e202301714.

[24] R. Walczak, A. Savateev, J. Heske, N. V. Tarakina, S. Sahoo, J. D. Epping, T. D. Kühne, B. Kurpil, M. Antonietti, M. Oschatz, *Sustain. Energy Fuels* **2019**, *3*, 2819.

[25] A. E. Bennett, C. M. Rienstra, M. Auger, K. V. Lakshmi, R. G. Griffin, *J. Chem. Phys.* **1995**, *103*, 6951.